

AN EVALUATION OF THE ACCURACY OF INVERTER SYNC ANGLE DURING THE GRID'S DISTURBANCES

Wojciech Jarzyna, Dariusz Zieliński, K. Gopakumar

- 1) Lublin University of Technology, Electrical Drive and Machine Department, ul. Nadbystrzycka 38A, 20-618 Lublin, Poland (✉ w.jarzyna@pollub.pl, +48 81 538 4341, d.zielinski@pollub.pl)
- 2) Indian Institute of Science, Department of Electronic Systems Engineering, Bangalore 560012, India (kgopa@iisc.ac.in)

Abstract

The grid-tied inverter synchronizes with the network on the basis of the instantaneous voltage phase angle. This angle is computed by the so-called synchronization algorithms. During grid disturbances, it is estimated with a certain accuracy, which varies for different disturbances and depends on the choice of algorithm. The tests presented here determine how to make an optimal selection of the synchronization algorithm. The research methods used are modeling, simulation and analysis of the results obtained. One of the most important outcomes is the determination of the root-mean-square sync error and its dynamics denotation. The research conclusions should be of particular interest to designers of distributed energy systems with a large number of inverter energy sources.

Keywords: inverter synchronization, synchronization angle, PLL, sync error, distributed grid.

© 2020 Polish Academy of Sciences. All rights reserved

1. Introduction

The synchronization of distributed energy sources which are connected to the electrical grid through power electronic converter requires precise identification of the instantaneous phase voltage angle. The determination of this angle causes no problem for an ideal power grid voltage characterizing a constant frequency and monoharmonic voltage shape. Unfortunately, in practice, such working conditions do not exist. Usually, the voltage in the power grid is distorted and the frequency may change slightly. Thus, accurate identification of the voltage phase angle plays a key role in the synchronization process and the quality of inverter operation.

Therefore, all generation systems connected to the power grid require accurate, continuous identification of the instantaneous phase angle. These systems include both large turbogenerators of conventional steam in coal power plants and hydrogenerators as well as distributed energy sources such as wind, diesel, photovoltaic and battery supplied micro-generators.

As shown in paper [12], regardless of the type of generator, the synchronization process requires very accurate identification of the instantaneous voltage phase angle. This angle corresponds to the angular path of the fundamental harmonic of the supply voltage. For a three-phase system (1) of power grid voltage $\mathbf{u}_g(t)$, or its equivalent notation $\mathbf{U}_{\alpha\beta}(t)$ in a two-phase $\alpha\beta$ frame (3) [16], the instantaneous synchronization angle (sync angle) is determined by the integral function (2) [9]:

$$\mathbf{u}_g(t) = \begin{bmatrix} u_A(t) \\ u_B(t) \\ u_C(t) \end{bmatrix} = \begin{bmatrix} U_{Am} \sin(\omega_g t) \\ U_{Bm} \sin(\omega_g t + 2\pi/3) \\ U_{Cm} \sin(\omega_g t + 4\pi/3) \end{bmatrix}, \quad (1)$$

$$\theta_g(t) = \int_0^t \omega_g dt, \quad (2)$$

$$\mathbf{U}_{\alpha\beta} = \begin{bmatrix} U_\alpha \\ U_\beta \end{bmatrix} = \mathbf{T}_{\alpha\beta} \mathbf{U}_{abc} = \frac{2}{3} \begin{bmatrix} 1 & -\frac{1}{2} & -\frac{1}{2} \\ 0 & \frac{\sqrt{3}}{2} & -\frac{\sqrt{3}}{2} \end{bmatrix} \begin{bmatrix} U_a \\ U_b \\ U_c \end{bmatrix}. \quad (3)$$

Due to the periodicity of trigonometric functions, the $\theta_g(t)$ angle of monoharmonic voltage takes a sawtooth shape corresponding to the instantaneous phase shift angle of the $u_\alpha(\omega_g t)$ voltage component (Fig. 1).

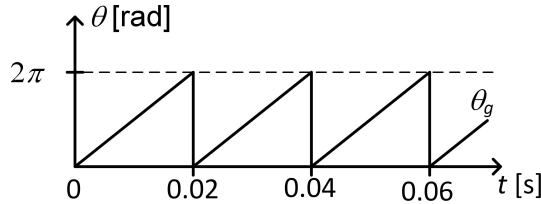


Fig. 1. Interpretation of the grid synchronization angle specified for a monoharmonic symmetrical voltage.

A generation system connected to the power grid must be synchronized with this network. Thus, in the remaining part of the paper, the instantaneous phase angle $\theta_g(t)$ is determined as the synchronization angle. The voltage of the exemplary micro-generator connected to the grid and its instantaneous phase angle is represented by the analogous formula as (1) and (2), with the difference that, instead of index g , index μ is applied to describe voltage $\mathbf{u}_\mu(t)$ and angle $\theta_\mu(t)$.

There are several methods that identify the synchronization angle. These methods include direct and indirect identification methods that use computational structures working in feedback or feedforward lines.

Indirect methods can have various computational complexity. The classic solution for three-phase systems is the *Synchronous Reference Frame Phase Locked Loop* (SRF PLL) algorithm [2, 3, 6, 22]. Its extensions use decomposition into positive and negative components [5] (e.g. *Double Decoupled Synchronous Reference Frame* DDSRF) [3], adaptive algorithms based on *Model Reference Adaptive Systems* (MRAS) [23], etc. [3, 6, 11, 13, 15, 23].

The choice of a synchronization algorithm depends on the type of disturbance and the tasks of the power electronic inverter, which includes active network support under the *Fault Ride Through* (FRT) grid codes [4, 10]. Meeting these tasks is especially important in distributed grids with a high amount of modern renewable energy generators.

However, despite the importance of synchronization, the choice of its algorithm is most often based on the expert knowledge of the designer. It is difficult to find information about objective methods of assessing synchronization algorithms. Therefore, the aim of this paper is the objectification of the assessment of synchronization algorithms. The research methods applied include mathematical modeling, computer simulation and analysis of results. The scope of work comprises an introduction to the synchronization of power electronic inverters, a brief description of synchronization algorithms, conducting simulation tests and their analyses, and the formulation of conclusions. The grid disturbances studied are especially dangerous for the stability of power grids [20], and concern voltage sags and incorrect switching of power lines in distribution power stations as well as higher harmonic impact in steady and instantaneous states.

2. Priorities of synchronization algorithms and measures of estimating the accuracy of the synchronization angle

It is most commonly accepted that the synchronization algorithm should produce the ideal saw-tooth instantaneous phase angle, regardless of the type of disturbance. The key demands to assess these requirements are:

- i) precise identification of the zero crossing of the first harmonic of the grid voltage and determination of the voltage frequency or period,
- ii) determination of voltage phase angle linearity,
- iii) identification of voltage phase angle delay.

Meeting these requirements allows active support of the power grid through collaborating micro-generators. Regardless of the type of disturbance, a three-phase symmetrical voltage is required at the output terminals of the inverter.

This paper investigates the meeting of i-iii conditions by various synchronization algorithms. The key value for this investigation is the synchronization error δ which is the input to determine the root mean square error (rms_{δ}). For several discussed disturbances and a selected group of synchronization algorithms, an analysis of the root mean square error and its changes over time was performed. The assessment of accuracy of the synchronization angle is closely related to the listed priorities. Therefore, the measure of the estimation of zero crossing and the first harmonic frequency are the estimates of angle $\delta(t)$ and rotation $\hat{\omega}(t)$. These estimates can change over time. The $\delta(t)$ error estimation can converge to zero or to another given level.

The incompatibility with the ideal saw-tooth shape of $\theta_{\mu}(t)$ may vary. The signal estimated can be shifted by a fixed value in reference to the $\theta_g(t)$ angle of the voltage grid (Fig. 2a). Disturbances also have a more complex form, as shown in Fig. 2b.

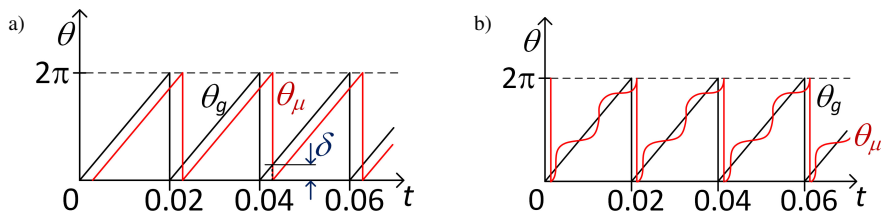


Fig. 2. Incompatibility of the estimated synchronization angle $\theta_{\mu}(t)$ of the micro-generator with the grid phase $\theta_g(t)$.
 a) constant angular displacement, b) angular displacement with additional oscillations $\theta_{\mu}(t)$.

The following measures were taken to assess the estimation accuracy of the synchronization angle:

- instantaneous value of the $\delta(t)$ phase error,

$$\delta(t) = \theta_g(t) - \theta_\mu(t), \tag{4}$$

where: $\theta_g(t)$ – instantaneous grid phase in a symmetrical voltage state, $\theta_\mu(t)$ – instantaneous phase of the micro-generator defined later in the paper as of the estimated sync angle. Moreover, the subscript “ μ ” is substituted by the name of the algorithm used: DSOGI, DDSRF, SRF and ATAN;

- root-mean-square rms_δ of the instantaneous value of the $\delta(t)$ phase error.

The instantaneous value of phase error $\delta(t)$ determines the inaccuracy of synchronization, and its graphic interpretation is shown in Fig. 2. This error allows the assessment of synchronization in both steady and transient states. The quasi-stationary measure is the root mean square error. This error calculated for the period T allows to determine if and how the rms_δ of the sync error changes over time. Its formula is defined in the same way as the formula for the rms current or voltage. Due to the symmetrical nature of the $\delta(t)$ error, in the paper rms_δ is computed for the 1/2 supply period. Thanks to this, it is possible to specify more precisely transient changes of $\delta(t)$ and the time after which the sync error is negligible.

$$rms_\delta = \sqrt{\frac{1}{T} \int_0^T (\delta(t))^2 dt}. \tag{5}$$

For an objective assessment of errors, it is preferable to use measures in the range [0; 1]. Such ranges are obtained for relative values, *i.e.* measures related to the base quantities. For angular measures with a small value, additional possibilities make angle representation by its sine function. For the tested cases, the estimated angles are very small on the order of several degrees. Hence, in expression (5) instead of the synchronization error δ , it is possible to determine the sinus function of this angle, *i.e.* $\sin(\delta)$. The obtained results of $\sin(\delta)$ measures are determined on a set of values from the range [-1; 1], and the root mean square error $rms_{\sin(\delta)}$ on the range [0; 1].

$$rms_{\sin(\delta)} = \sqrt{\frac{1}{T} \int_0^T [\sin(\delta(t))]^2 dt}. \tag{6}$$

This method gives good results for small angles δ , hence it can be used to estimate synchronization errors. In the computational program, variables are designated according to a description shown in Table 1.

Table 1. Designation of variables and indicators used in the computational program (Matlab).

Variable description	Variable	Designation in the computational program
synchronisation angle	$\theta(t)$	theta
synchronisation error	$\delta(t)$	delta
root mean square error	$rms_{\sin(\delta)}$	rms(delta)
response time	–	delay

3. Synchronization algorithms

The number of synchronization algorithms applied in power electronic converters is very large [1–4]. For three-phase networks, one can distinguish algorithms based on zero-crossing detection, operation in open-loop systems, or in closed-loop systems. The first of these systems, based on zero-crossing detection, is not resistant to disturbances. It is sensitive to accidental zero crossings and cannot estimate the synchronization angle online. Its maximal synchronization errors can reach a value close to the voltage period. The other two types of algorithms, operating in open as well as in closed loop systems, are used in various configurations, such as: low and band-pass filter [3], weighted least square estimation [6], notch filter or resonant filter [19] or trigonometric filters [8]. They can be an attractive alternative, especially due to short computation time.

The closed-loop algorithms offer more advanced possibilities. They can operate with high accuracy even in asymmetric or nonlinear conditions. Among many different structures, the most frequently described algorithms include *Synchronous Reference Frame Phase Locked Loop* (SRF-PLL) [1, 7, 21], *Double Synchronous Reference Frame or Double Decoupled Synchronous Reference Frame* (DDSRF PLL) [17], *Second-Order Integrator* (SOGI PLL) and *Double Second-Order Integrator* (DSOGI PLL) [16, 17], Robust PLL [17] or adaptive algorithms. Out of the mentioned synchronization algorithms, the four most often used were selected for the tests in question *i.e.* SRF-PLL – Synchronous Reference Frame Phase Locked Loop, ATAN – Arc Tangent filter estimating the synchronization angle based on the space vector in the $\alpha\beta$ reference frame, DDSRF PLL – Double Decoupled Synchronous Reference Frame Phase Locked Loop and DSOGI PLL – Double Second-Order Generalized Integrator PLL.

Parameters of the SRF-PLL, DDSRF and DSOGI regulator algorithms have been tuned in accordance with the guidelines of optimal settings, which are described in the scientific literature and academic textbooks [1, 21, 24]. They consistently indicate that the optimal settings are selected by tuning the damping factor ζ and the settling time T_s , described in detail among others by a team from the Aalborg University of Technology [1, 21]. It can, obviously, happen that under specific disturbance conditions and modifications of the control aims, the controller settings should be changed. However, such a research task goes beyond the purpose of the present article. It is expected that the problem in question will be addressed in a follow-up study by the authors.

3.1. Synchronous Reference Frame PLL

The basic algorithm for the synchronization of three-phase voltages is the SRF-PLL shown in Fig. 3a where the instantaneous value of the phase angle is detected by synchronization of the rotating reference frame with the power grid voltage vector. The SRF-PLL algorithm uses variables received after the application of the Clarke transformation, which converts a natural abc frame into an $\alpha\beta$ two-phase frame, and then the Park transformation converting $\alpha\beta$ into a rotating dq frame. The position of a grid angle is obtained by setting the U_q at zero and then the result of the comparison is processed by a PI controller. The estimated synchronization speed ω_θ after adding grid frequency ω_0 and integration of the result generates the $\theta_{PLL}(t)$ sync angle with a grid saw-tooth shape for sinusoidal and symmetrical grid voltages.

3.2. Double Decoupled Synchronous Reference Frame PLL

As in SRF-PLL, in this algorithm (Fig. 3b) the instantaneous value of the grid voltage phase angle is detected by synchronization of a rotating reference frame with the grid voltage vector.

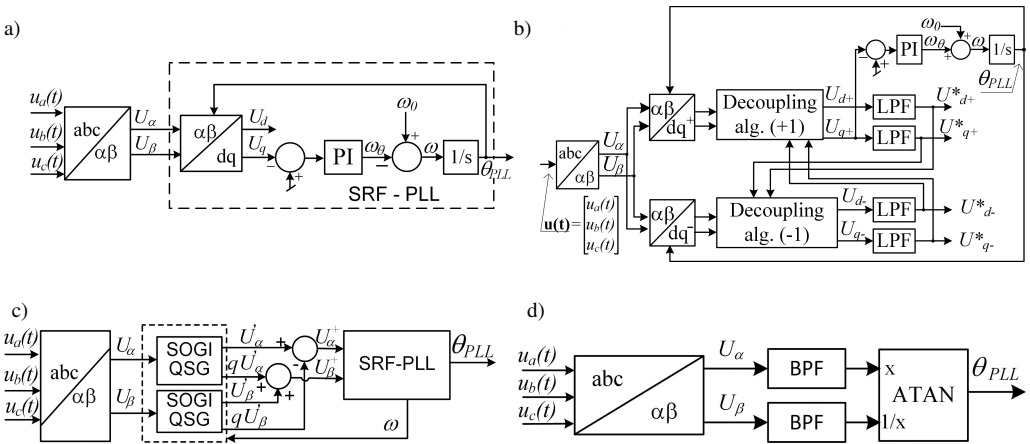


Fig. 3. Synchronization algorithms considered in the paper: a) Synchronous Reference Frame SRF-PLL; b) Double Decoupled Synchronous Reference Frame DDSRF; c) Double Second-Order Generalized Integrator DSOGI PLL, where QSG are Quadrature Signal Generators; d) ATAN simplified Tangent filter algorithm.

The approach is also based on the coordinate transformation from abc to $\alpha\beta$, and then from $\alpha\beta$ to dq . The main difference is the use of the positive sequence voltage component. To achieve this, two transformations are introduced which transfer variables to systems rotating in positive $dq+$ and negative $dq-$ sequences. Based on the results of the $T_{\alpha\beta/dq+}$ transformation and thanks to the decoupling algorithm, the synchronization angle $\theta(t)$ can be determined according to the classic SRF PLL algorithm. Such actions allow estimating the sync signal even with the presence of asymmetrical voltages. However, due to a large number of computations, the processing time is definitely longer than that of the classic SRF PLL.

3.3. Double Second Order Generalized Integrator PLL

One of the most frequently applied alternative synchronization algorithms is the *Double Second-Order Generalized Integrator PLL* (DSOGI), shown in Fig. 3c. Unlike the DDSRF-PLL algorithm, the components of the voltage spatial vector are filtered in the $\alpha\beta$ stationary system and not in the rotating system dq . Filtrations are carried out by two resonant filters shifted to each other by 90 deg, which removes negative voltage components. From here, only the positive component vector is fed to the SRF-PLL input.

3.4. Arc Tangent filter ATAN

The algorithm (Fig. 3d) belongs to the group of estimators working without a feedback loop. It operates on variables in the $\alpha\beta$ stationary frame. In its structure, the perpendicular voltage paths α and β are filtered. After this action, voltages are fed to the inputs of the Arc Tangent block which calculates the sync angle $\theta(t)$.

This type of algorithm is only useful in cases where the three-phase signal of the network is symmetrically balanced. The advantages of this solution are short computation time and simplicity of implementation.

4. Sync angle estimation tests and their accuracy analysis

As mentioned in section 2, selected synchronization algorithms were tested against disturbance on the step phase change of the voltage grid, single-phase short-circuit and two-phase short-circuit. Four types of synchronization algorithms, SRF-PLL, ATAN, DDSRF PLL, and DSOGI PLL were studied. The object of the research was a photovoltaic micro-generator which was coupled to the power grid via a vector controlled inverter with the Voltage Oriented Control system (Fig. 4).

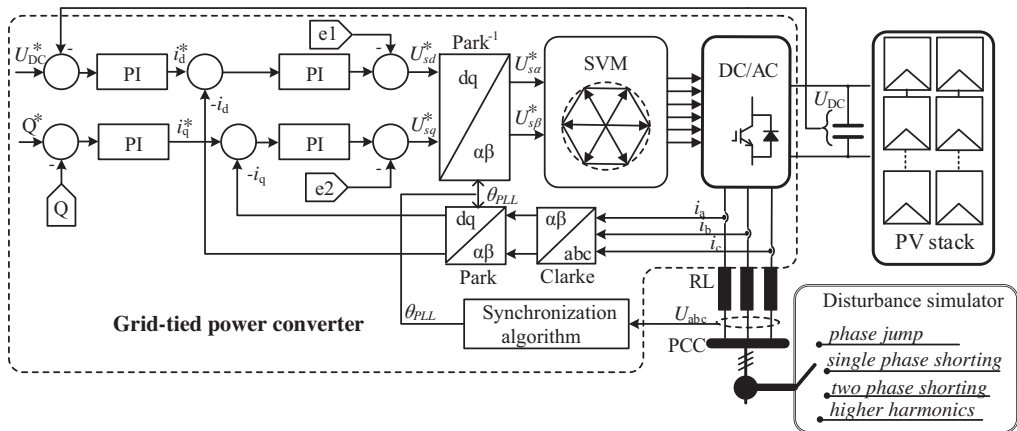


Fig. 4. Simplified diagram of a photovoltaic micro-generator connected to a grid by a VOC inverter with switchable synchronization algorithms and simulated disturbances in the power grid.

Computational research was carried out in the Matlab Simulink program. The results of each test are presented in the graphical form showing instantaneous phase angle $\theta_g(t)$ and inverter synchronization angle $\theta_\mu(t)$, instantaneous error $\delta(t)$ and root mean square error value $rms_{\sin \delta}$. The cumulative comparative values of the root mean square errors for all the samples are presented in the form of histograms shown in section 5.

In the computational program, variables are designated according to the description shown in Table 2.

Table 2. Designation of variables and indicators in the applied computational program Matlab.

Variable description	Variable	Designation in the computational program
synchronization angle	$\theta(t)$	Theta
synchronization error	$\delta(t)$	delta
root mean square error	$rms_{\sin(\delta)}$	rms(delta)

4.1. Effect of a phase angle step change on the accuracy of sync angle estimation

A step-change in the phase angle can happen as a result of switching the power line. If the angle reaches several degrees, then this deviation can be caused by a different parameters of the switched transmission line. If the angle is about 30 degrees or a multiple of this value, then the

source of such a large shift is caused by a different group coupling the transformers supplying the lines. For example, switching from Dz6 to Dy5 is accompanied by a step-change in a three-phase voltage shift of 30 degrees. Such a case was considered during the research and it is illustrated in Fig. 5.

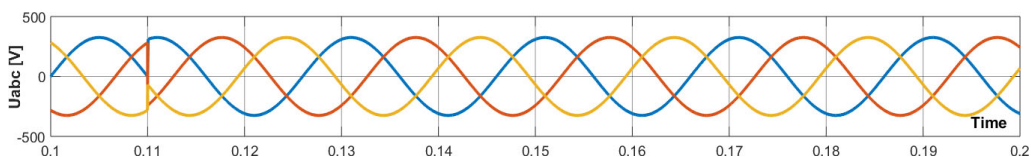


Fig. 5. A 30-degree phase step of the U_{abc} voltage being the consequence the DZ6 to Dy5 switching at $t = 0.11$ s.

This switching qualifies for an emergency event. Its impact on the operation of the inverter can be assessed on the basis of synchronisation errors. Figures 6a–d and 7a–d show the obtained synchronisation results.

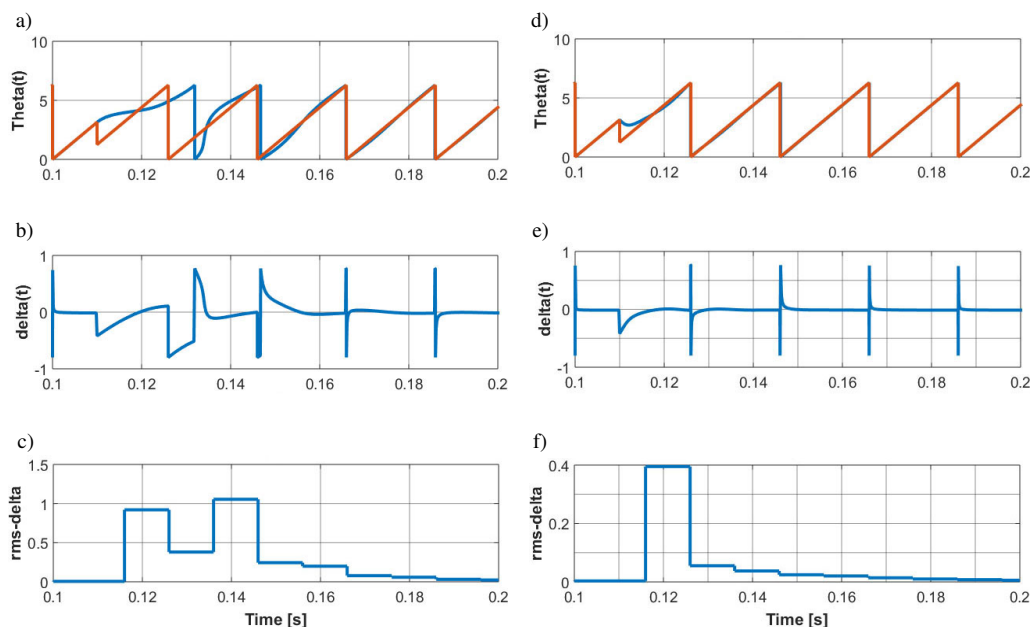


Fig. 6. The impact of a 30-degree phase step on the synchronisation angle $\theta(t)$ (Theta(t) in the figure), sync error $\delta(t)$ (delta(t)) and the root mean square of error rms_{δ} during synchronisation using the following algorithms: DSOGI PLL – graphs a)÷c); DDSRF PLL – graphs d)÷f).

For the estimated synchronization angle, the traces of the grid phase angle θ_g and the sync angle θ_{μ} estimated by algorithms ATAN and SRF PLL overlap, so in Fig. 6a and Fig. 6d only one line is visible. This is confirmed by an almost imperceptible error in the delta diagram – b) and e) and rms (delta) in diagrams c) and f). In the case of the classic SRF PLL algorithm, a noticeable error occurs only for the first half-cycle of the disturbance. In subsequent periods, the error practically decreases to zero. The peaks in Fig. 7e) result from numerical processing and due to their very short duration are not even visible in rms calculations and are of no practical importance.

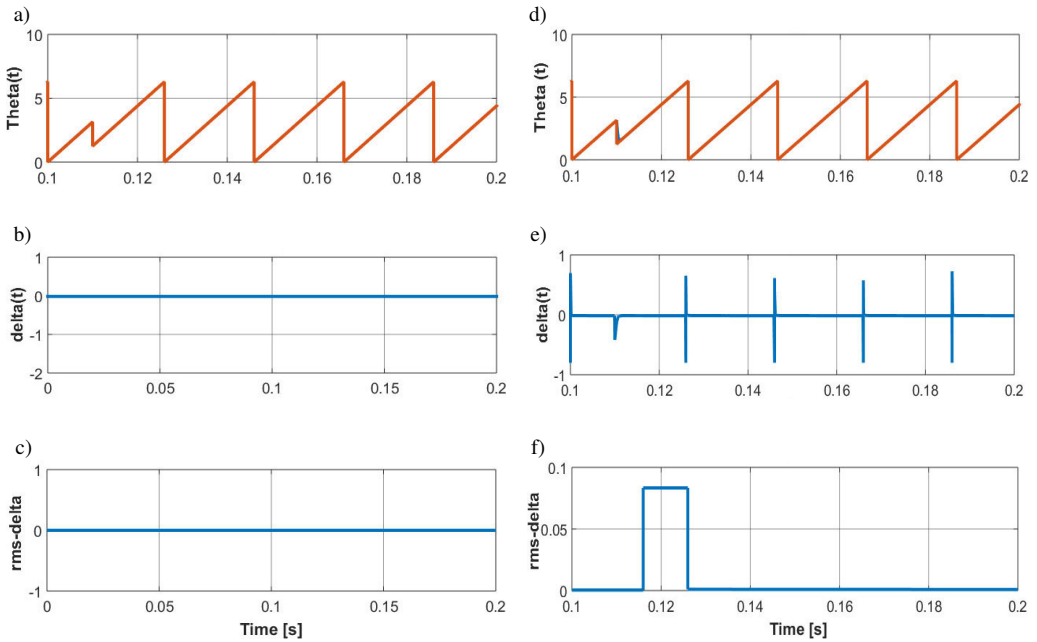


Fig. 7. The impact of a 30-degree phase step on the synchronisation angle $\theta(t)$ (Theta(t) in the figure), sync error $\delta(t)$ (delta(t) in the figure) and the root mean square of error rms_{δ} during synchronisation using the following algorithms: ATAN – graphs a)÷c); SRF PLL – graphs d)÷f).

4.2. Effect of a single-phase short circuit on the accuracy of sync angle estimation

The single-phase short circuit considered takes place during short-circuits in four-wire networks and happens during the connection of any line phase with a neutral line (Fig. 8).

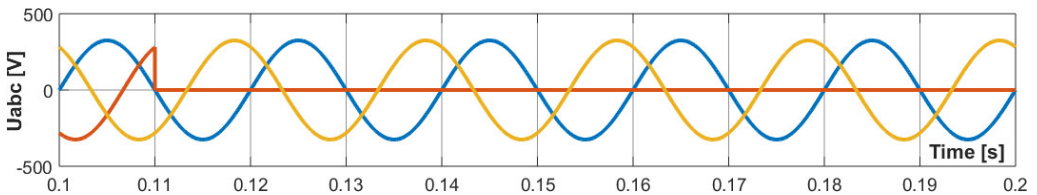


Fig. 8. The L2 line short circuit to zero potential wire.

For this type of transient short circuit, the operating conditions must survive for the time specified in the FRT codes of the grid operator. In the time required by these codes, active participation in voltage recovery is required. This is why the full capacity of inverters to generate symmetrical voltage is so important and correct synchronization is essential for obtaining such a property. How individual synchronization algorithms implement this is shown in Figs. 9a–f and Figs. 10a–f.

During a short circuit, the DSOGI PLL and DDSRF PLL synchronization the rms_{δ} errors converge to zero (Fig. 9). It follows that inverters with these algorithms actively support the electric grid during single-phase short-circuits.

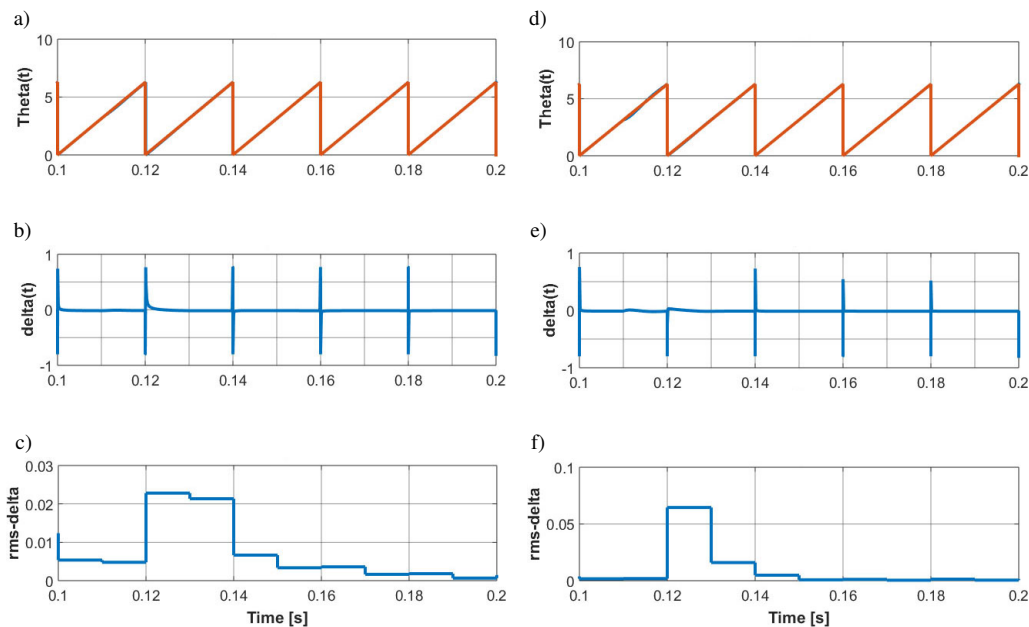


Fig. 9. The impact of a single-phase short-circuit on the synchronisation angle $\theta(t)$ (Theta(t) in the figure), sync error $\delta(t)$ (delta(t) in the figure) and the root mean square of error rms_{δ} during synchronisation using the following algorithms: DSOGI PLL – graphs a)÷c); DDSRF PLL – graphs d)÷f).

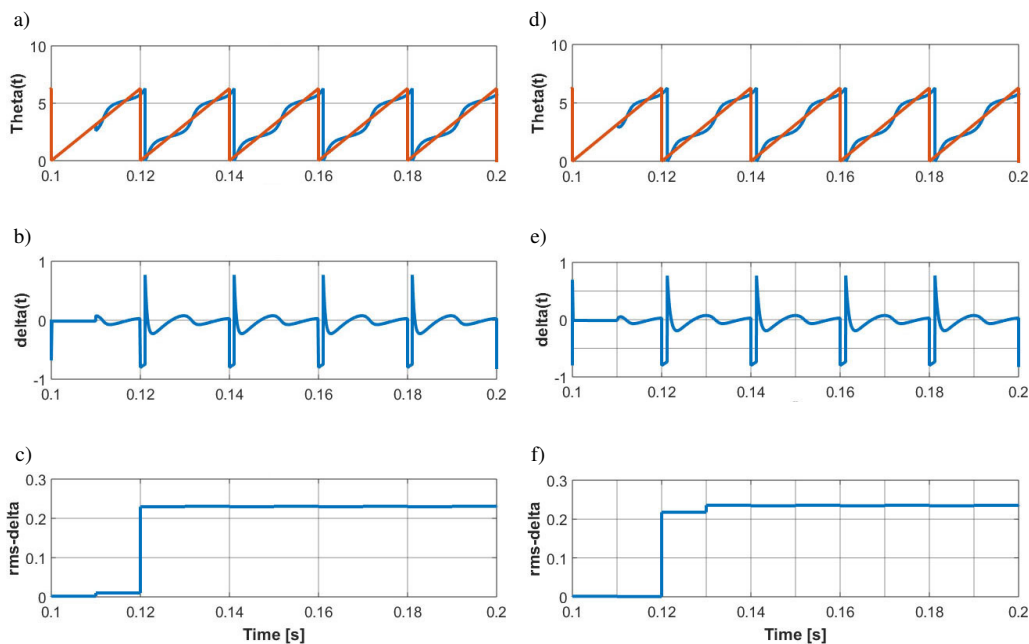


Fig. 10. The impact of a single-phase short-circuit on the synchronisation angle $\theta(t)$ (Theta in the figure), sync error $\delta(t)$ (delta in the figure) and the root mean square of error rms_{δ} during synchronisation using the following algorithms: ATAN – graphs a)÷c); SRF PLL – graphs d)÷f).

The root mean square error for the ATAN and SRF PLL algorithms indicates that the rms_{δ} error never decreases to zero (Fig. 10). Therefore, with single-phase short-circuits, neither of the algorithm supports the network in response to a symmetrical three-phase supply voltage.

4.3. Effect of a two-phase short circuit on the accuracy of sync angle estimation

In the course of the analysis, it was assumed that a two-phase short circuit is a direct connection of two phases.

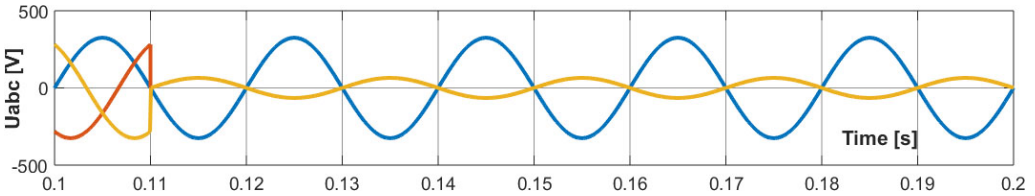


Fig. 11. Voltage during a direct short circuit of two phases L2 and L3.

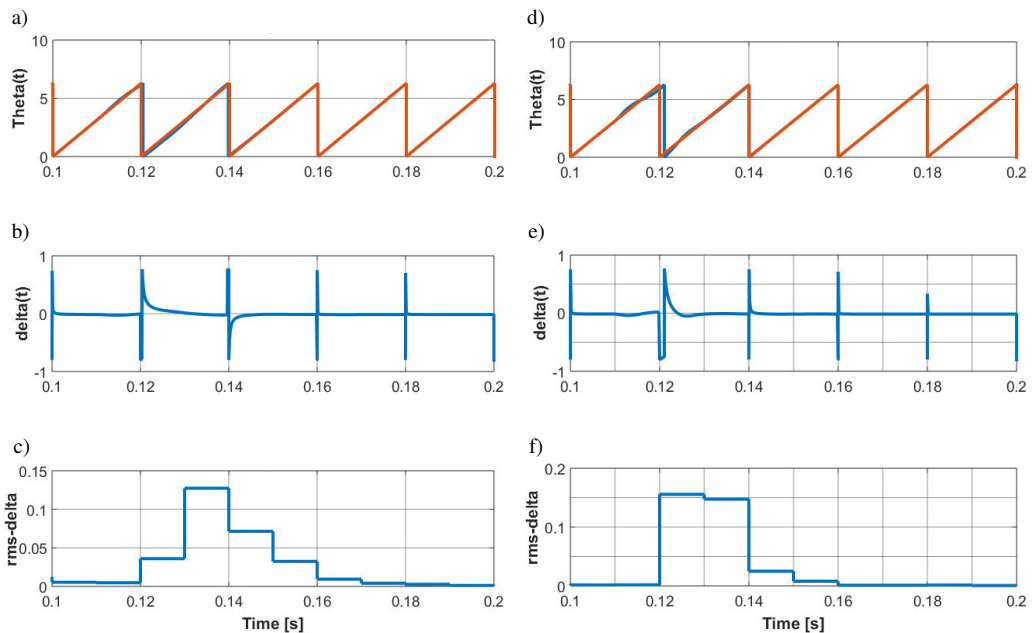


Fig. 12. The impact of a two-phase short-circuit on the synchronisation angle $\theta(t)$ (Theta(t)) and the sync error $\delta(t)$ (delta(t)) and the root mean square of error rms_{δ} during synchronisation using the following algorithms: DSOGI PLL – graphs a)÷c); DDSRF PLL – graphs d)÷f).

Similarly to a single-phase short-circuit, the use of synchronization algorithms SRF PLL and ATAN leads to a constant high value of synchronization errors. Therefore, this solution does not meet the conditions for correct operation of micro-generators supporting the electric grid. In contrast, the advanced DSOGI PLL and DDSRF PLL algorithms overcome this short circuit very well.

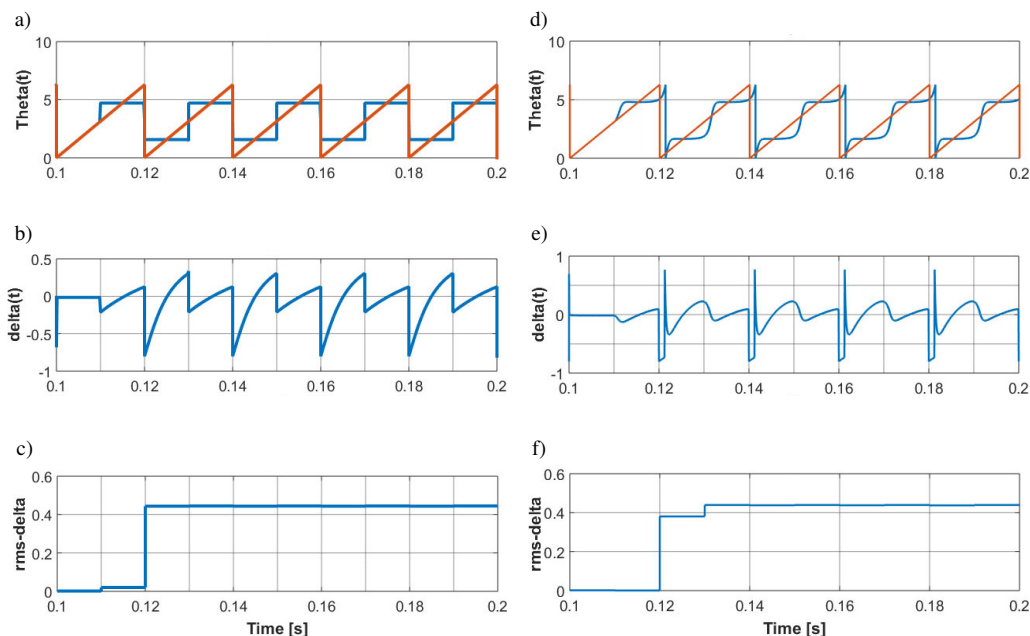


Fig. 13. The impact of a two-phase short-circuit on the synchronisation angle $\theta(t)$ (Theta(t) in the figure), sync error $\delta(t)$ (delta(t) in the figure) and the root mean square of error rms_{δ} during synchronisation using the following algorithms ATAN – graphs a)÷c); SRF PLL – graphs d)÷f).

4.4. Impact of unbalanced load on grid disturbed by higher harmonics

The synchronization algorithms used in the present research operate with high accuracy during disturbances caused by higher harmonics of voltage at symmetrical three-phase grid voltages. This is documented by research results conducted among others at the universities of Aalborg, Barcelona, Napoli, Warsaw and Lublin [1–3, 9, 13, 16–18]. However, if the three-phase voltage system does not meet the symmetry conditions, the operating conditions definitely deteriorate, and the accuracy of the synchronization angle estimation can be laden with an error.

During the implementation of such asymmetrical conditions, an assumption was made that the power grid is loaded by a power electronic converter, e.g. a station for charging electric vehicles. It was assumed that with a symmetrical load the level of distortion by the fifth harmonic is 7.8%, by the seventh harmonic – 3.2%, and the *total harmonic ratio of voltage distortion* equals $THDu = 8.6\%$. After a double overloading of one of the power phases, an unbalanced three-phase voltage system was created. As a result, the third harmonic with 9.8%, the fifth harmonic with 8.9% and the seventh harmonic with 4.2% were identified in the line voltage, and the $THDu$ was 14.3%. For these conditions, similarly to previous cases, simulation tests were carried out, the results of which are presented in Figs. 14–16. During the simulation tests, an initial state with a symmetrical voltage system was predicted (Fig. 14, time from 0.1 to 0.11). At $t = 0.11$ s, an unbalanced step load was generated which resulted in the above-mentioned unbalanced voltage system.

Based on the obtained results, it can be stated that the synchronization algorithms tested determine the angle of synchronization with a high degree of accuracy even if there occurs a significant deformation of higher voltage harmonics. The accuracy level of the estimated

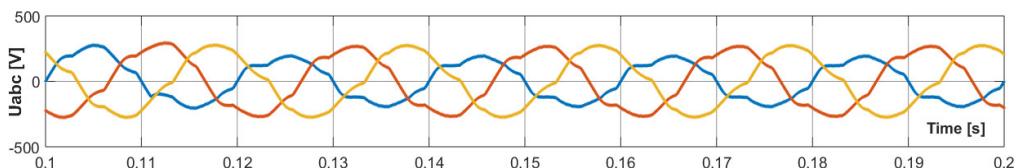


Fig. 14. Voltage in the presence of higher harmonics.

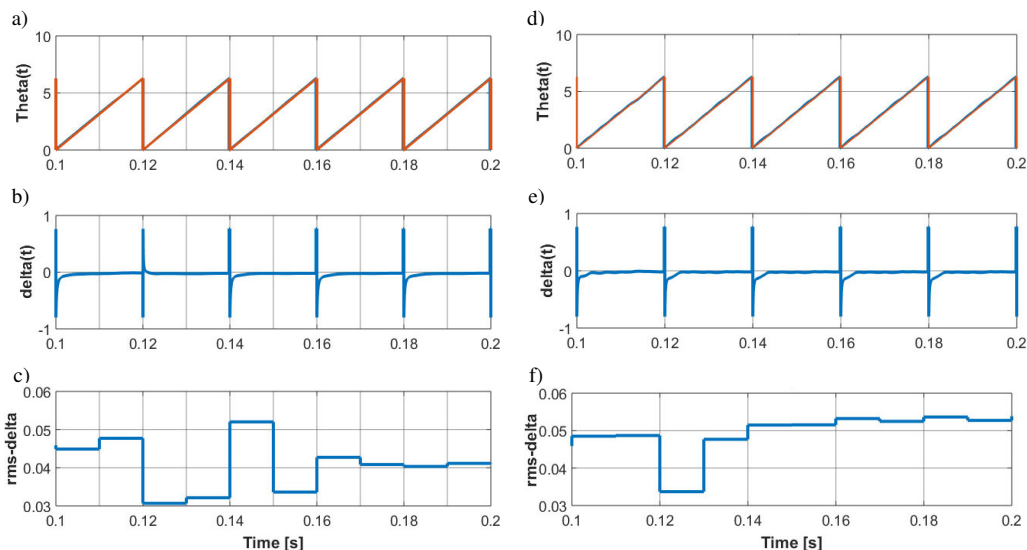


Fig. 15. The impact of a higher harmonic on the synchronisation angle $\theta(t)$ (Theta(t), sync error $\delta(t)$ (delta(t)) and the root mean square of error rms_{δ} during synchronisation using the following algorithms: DSOGI PLL – graphs a)÷c); DDSRF PLL – graphs d)÷f).

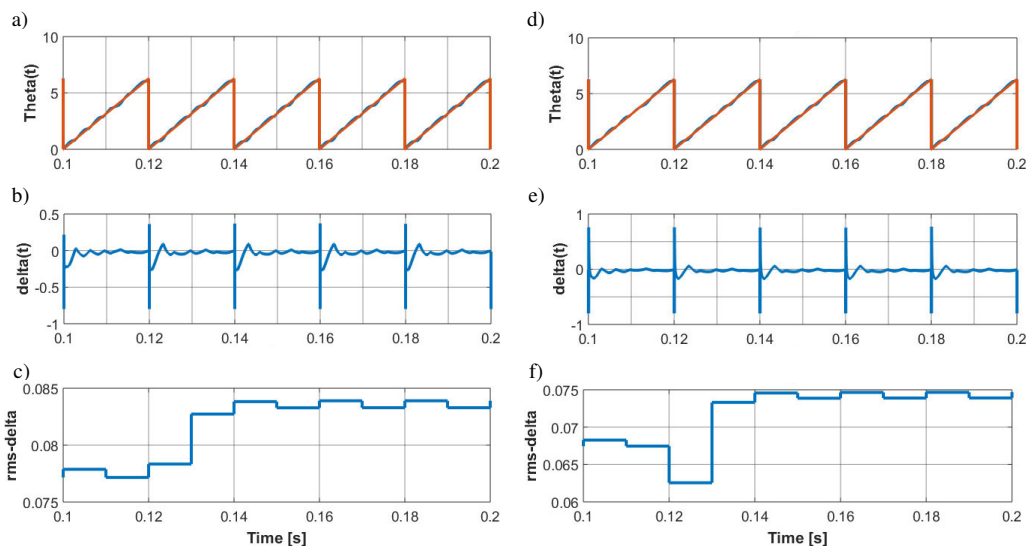


Fig. 16. The impact of a higher harmonic on the synchronisation angle $\theta(t)$ (Theta(t) in the figure), sync error $\delta(t)$ (delta(t) in the figure) and the root mean square of error rms_{δ} during synchronisation using the following algorithms: ATAN – graphs a)÷c); SRF PLL – graphs d)÷f).

synchronization angle, determined by the rms root mean square error, was in the range of 5–7%. Even a rapid increase in the deformation level, produced by unbalanced grid voltages, did not cause significant changes and remained within the range of 4 to 8.5% rms. As was to be expected, during voltage unbalance the synchronization angle was best estimated by the DSOGI and DDSRF algorithms which showed by far the best results in all the states of power grid asymmetry considered in this study.

5. Analysis and evaluation of the results received

In order to compare the results presented in Figs. 5 to 16, bar charts in Fig. 17 show the maximum and final values of $rms_{\sin(\delta)}$ errors for the considered disorders. In this graph, the blue bars indicate the maximum error, and the red bars specify the error at the end of the simulation time.

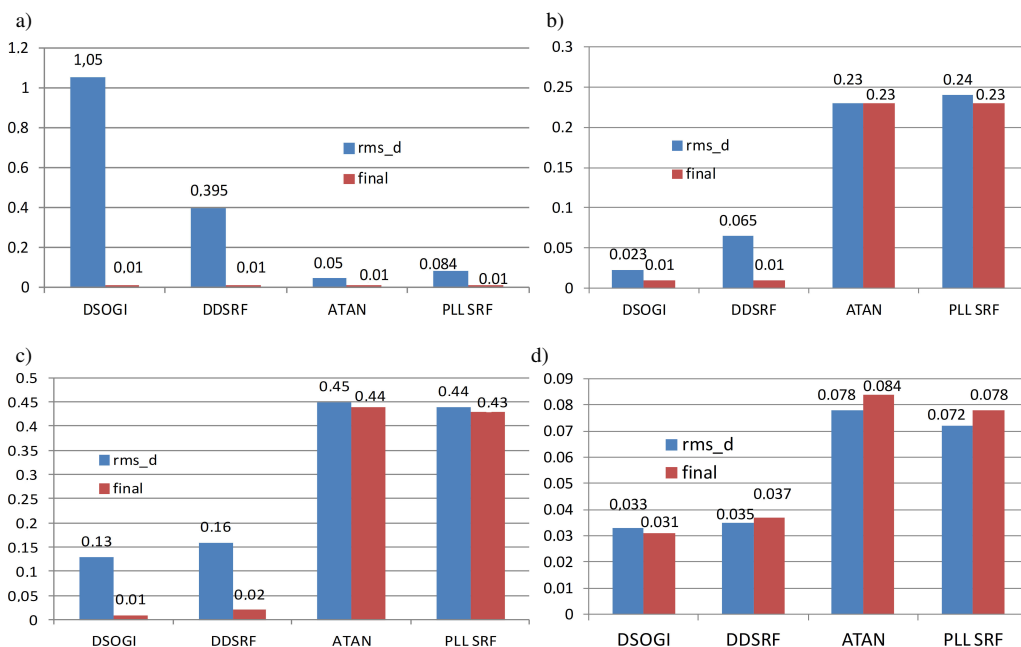


Fig. 17. An evaluation of the accuracy of synchronization angle estimation during an event as: a) phase jump, b) single-phase short-circuit, c) two-phase short-circuit, d) higher harmonic disturbances; where: rms_d – specifies maximal value of the $rms_{\sin(\delta)}$, final – specifies final value of the $rms_{\sin(\delta)}$ at the end of simulation time.

Based on the presented results, it is clearly seen that the DSOGI and DDSRF algorithms achieve very good results both in the assessment of the maximum level of interference and steady-state. Only in the case of a phase jump the initial values are much higher for these algorithms. However, this error is not dangerous for converters, due to the high dynamics of the synchronization causing the error to fall almost to zero and limiting the active current, which protects the converter and the micro-source against an excessive increase of line current.

As expected, the worst conditions occur with unsymmetrical voltage sags. The presented assessment method confirms this. The danger lies in the fact that synchronization errors for the

SRF PLL and ATAN algorithms do not go down to zero. This can be a serious problem with meeting the FRT conditions of a grid operator [4, 10].

The last chart, Fig. 17d, confirms that higher harmonics produce synchronization errors and in addition, asymmetrical non-linear loads increase these errors. The error rate for these disorders is stable and does not decrease as a function of time. When analyzing error levels in Fig. 17d, it should be noted that the scale on the vertical ordinate axis is more than five times smaller than in the adjacent graph 17.c and, therefore, the maximum errors are accordingly smaller. This confirms that advanced DSOGI and DDSRF algorithms work effectively even during a higher harmonic disturbance.

6. Summary

The analysis presented here is based on the error root mean square $rms_{\sin(\delta)}$, its changes in time and the temporary error $\delta(t)$ itself. On its basis, it can be concluded that the correctness of the adopted method of objectification of the measure and assessment of the accuracy of the estimated synchronization angle has been proved. This fact, therefore, confirms the implementation of the research objective of this paper.

The above statement results from the analysis of the outcomes. The cases shown refer to disorders of a different nature and causing different effects. The algorithms used are representative examples and some of the most commonly used in control systems of grid-tied inverters. The proposed method allows to determine instantaneous synchronization errors $\delta(t)$ and then the $rms_{\sin(\delta)}$. Using the values computed in this way, it is possible to formulate evaluations of individual algorithms in relation to the type of disturbance. It is also very important that these assessments prove the results of scientific research, which confirms the validity of the method applied to assess the accuracy of the synchronization estimation.

The proposed assessments can be extended to other algorithms and disturbances. Their further analysis is the subject of the authors' broader scientific studies, in which the simulation results will be verified in a real laboratory set-up.

Acknowledgements

This work was supported under the project "Electric vehicle energy transfer system integrated with lighting infrastructure – PLUGinEV" of the Polish National Centre for Research and Development, project No. POIR.04.01.02-00-0052/16.

References

- [1] Teodorescu, R., Liserre, M., Rodriguez, P. (2011). *Grid Converters for Photovoltaic and Wind Power Systems*. Chichester: John Wiley & Sons Ltd.
- [2] Bobrowska-Rafal, M., Rafal, K., Jasinski, M., Kazmierkowski, M. (2011). Grid synchronization and symmetrical components extraction with PLL algorithm for grid connected power electronic converters – a review. *Bulletin of the Polish Academy of Sciences Technical Sciences*, 59(4), 485–497.
- [3] Blanco, C., Reigosa, D., Briz, F., Guerrero, J.M., García, P. (2012). Grid synchronization of three-phase converters using cascaded complex vector filter PLL. *Proc. of 2012 IEEE Energy Conversion Congress and Exposition (ECCE)*, 196–203.

- [4] ENTSO-E AISBL, *ENTSO-E: Network Code for Requirements for Grid Connection Applicable to all Generators*, Brussels, 8 March 2013.
- [5] Baradarani, F., Zadeh, M.R.D., Zamani, M.A. (2014). A phase-angle estimation method for synchronization of grid-connected power-electronic converters. *IEEE Transactions on Power Delivery*, 30(2), 827–835.
- [6] Liccardo, F., Marino, P., Raimondo, G. (2010). Robust and fast three-phase PLL tracking system. *IEEE Transactions on Industrial Electronics*, 58(1), 221–231.
- [7] Hans, F., Schumacher, W., Harnefors, L. (2017). Small-signal modeling of three-phase synchronous reference frame phase-locked loops. *IEEE Transactions on Power Electronics*, 33(7), 5556–5560.
- [8] Freijedo, F.D., Yepes, A.G., Lopez, O., Fernandez-Comesana, P., Doval-Gandoy, J. (2011). An optimized implementation of phase locked loops for grid applications. *IEEE Transactions on Instrumentation and Measurement*, 60(9), 3110–3119.
- [9] Jarzyna, W. (2019). A survey of the synchronization of synchronous generators and power electronic converters, *Bulletin of the Polish Academy of Sciences: Technical Sciences*, 67(6), 1069–1083.
- [10] Jarzyna, W., Lipnicki, P. (2013). The comparison of Polish grid codes to certain European standards and resultant differences for WPP requirements. *Proc. of 2013 15th European Conference on Power Electronics and Applications (EPE)*, 1–6.
- [11] Zieliński, D., Lipnicki, P., Jarzyna, W. (2015). Synchronization of voltage frequency converters with the grid in the presence of notching. *Compel: International journal for computation and mathematics in electrical and electronic engineering*, 34(3), 657–673.
- [12] Jarzyna, W., Zieliński, D., Zielińska, K., Fatyga, K. (2017). Reduction of voltage and power oscillation in the two-phase shorting of a grid inverter. *Proc. of 2017 19th European Conference on Power Electronics and Applications (EPE'17 ECCE Europe)*.
- [13] Liccardo, F., Marino, P., Schiano, C., Visciano, N. (2004). A New Robust Phase Tracking System for Asymmetrical and Distorted Three Phase Networks. *Proc. of 2004 11th International Conference on Harmonics and Quality of Power*, 525–530.
- [14] Lipnicki, P. (2014). Comparison of performance of synchronization algorithms for grid connected power electronics converters according to proposed evaluation quality criteria. *Informatyka, Automatyka, Pomiary w Gospodarce i Ochronie Środowiska*, (1), 62–65.
- [15] Menxi Xie, Canyan Zhu, Liqun He, Huiqing Wen. (2017). An Experimental Study of MAF-SRF-PLL with Comb Compensator. *Proc of 2017 IEEE Applied Power Electronics Conference and Exposition (APEC)*, 1310–1313.
- [16] Rodriguez, P., Luna, A., Munoz-Aguilar, R.S., Etxeberria-Otadui, I., Teodorescu, R., Blaabjerg, F. (2012). A Stationary Reference Frame Grid Synchronization System for Three-Phase Grid-Connected Power Converters Under Adverse Grid Conditions. *IEEE Transactions on Power Electronics*, 27(1), 99–112.
- [17] Rodriguez, P., Pou, J., Bergas, J., Candela, J.I., Burgos, R.P., Boroyevich, D. (2007). Decoupled double synchronous reference frame PLL for power converters control. *IEEE Transactions on Power Electronics*, 22(2), 584–592.
- [18] Rodriguez, P., Teodorescu, R., Candela, I., Timbus, A.V., Liserre, M., Blaabjerg, F. (2006). New positive-sequence voltage detector for grid synchronization of power converters under faulty grid conditions. *Proc. of 2006 37th IEEE Power Electronics Specialists Conference*.
- [19] Rauth, S.S., Kumar, M., Srinivas, K. (2018). A Proportional Resonant Power Controller and A Combined Amplitude Adaptive Notch Filter with PLL for Better Power Control and Synchronization of Single Phase On Grid Solar Photovoltaic System. *Proc. of 2018 International Conference on Smart Systems and Inventive Technology (ICSSIT)*, 378–384.

- [20] Szcześniak, P., Kaniewski, J. (2015). Hybrid transformer with matrix converter. *IEEE Transactions on Power Delivery*, 31(3), 1388–1396.
- [21] Timbus, A., Liserre, M., Teodorescu, R., Blaabjerg, F. (2005). Synchronization methods for three phase distributed power generation systems – An overview and evaluation. *Proc. of 2005 IEEE 36th Power Electronics Specialists Conference*, 2474–2481.
- [22] Kaura, V., Blasko, V. (1997). Operation of a phase locked loop system under distorted utility conditions. *IEEE Transactions on Industry Applications*, 33(1), 58–63.
- [23] Wang, Y.F., Li, Y.W. (2010). Grid synchronization PLL based on cascaded delayed signal cancellation. *IEEE Transactions on Power Electronics*, 26(7), 1987–1997.
- [24] Dong, D., Wen, B., Boroyevich, D., Mattavelli, P., Xue, Y. (2014). Analysis of phase-locked loop low-frequency stability in three-phase grid-connected power converters considering impedance interactions. *IEEE Transactions on Industrial Electronics*, 62(1), 310–321.